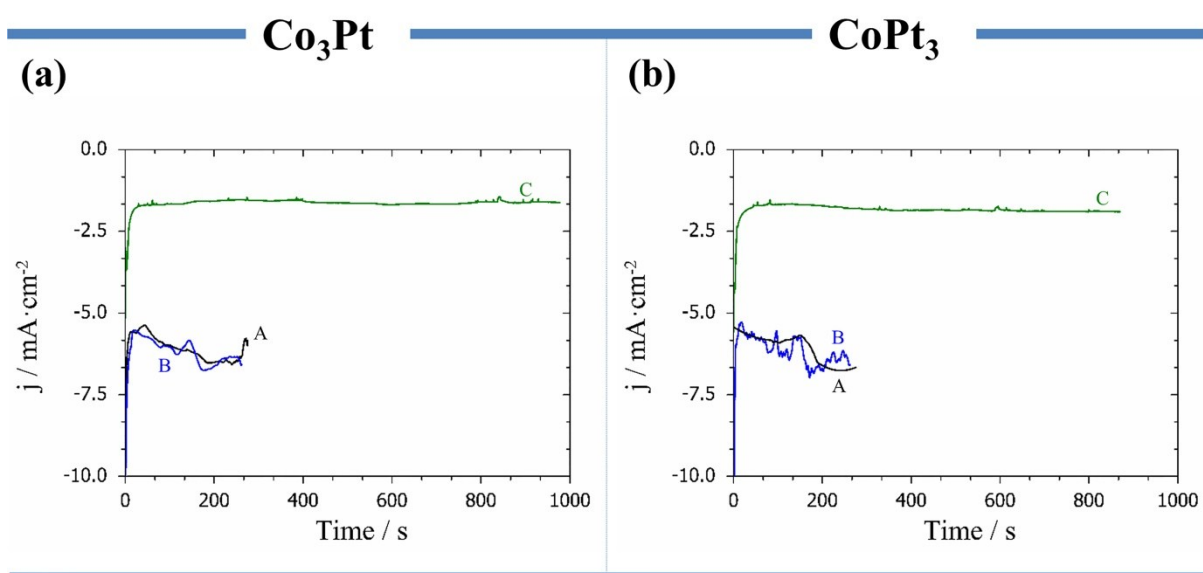


## Effective ionic-liquid microemulsion based electrodeposition of mesoporous Co-Pt films for methanol oxidation catalysis in alkaline media

Albert Serrà,<sup>a</sup> Elvira Gómez,<sup>a</sup> Igor V. Golosovsky,<sup>b</sup> Josep Nogués,<sup>c,d</sup> and Elisa Vallés<sup>a,\*</sup>

### Cronoamperometric curves of the films electrosynthesis

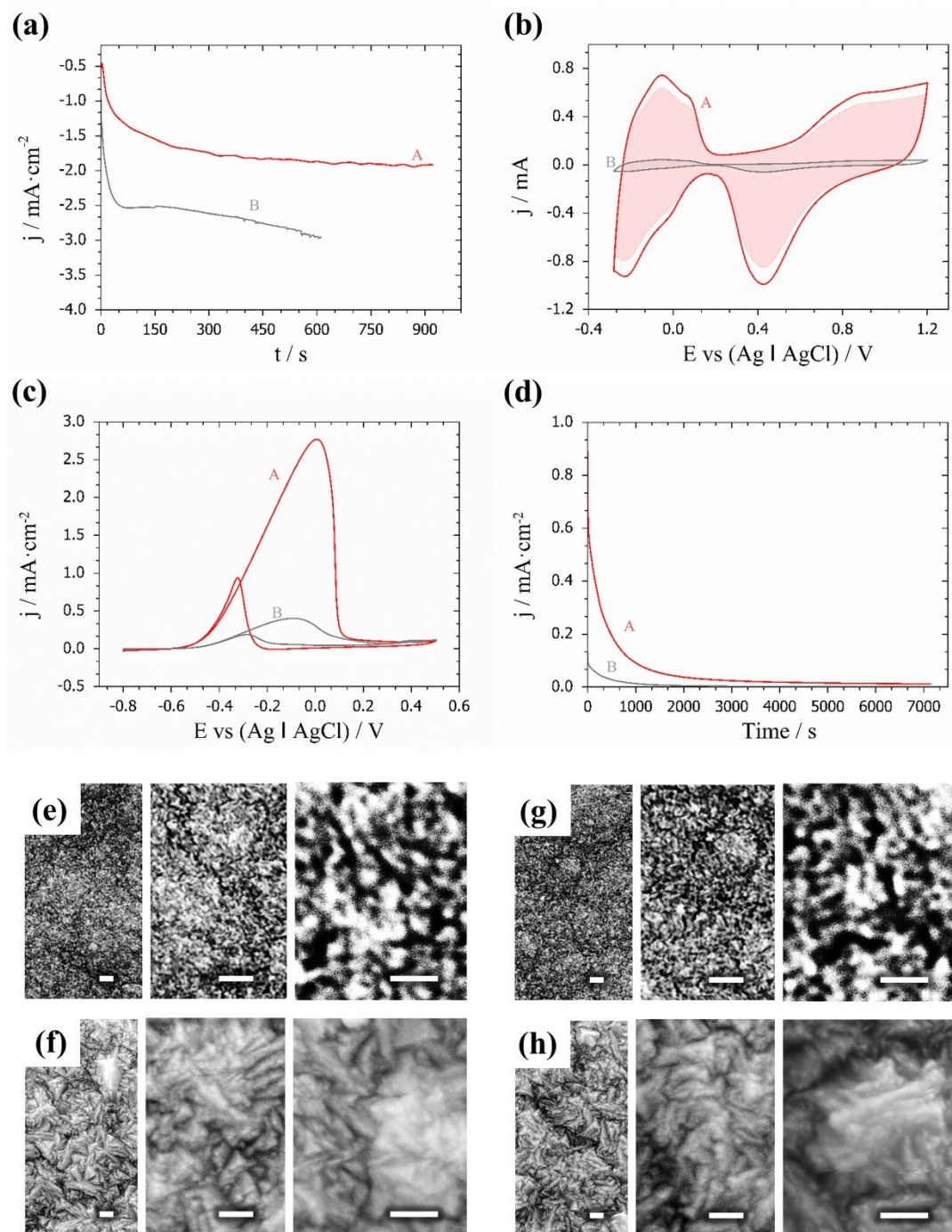


**Fig. 1S:** Cronoamperometric curves of the (a)  $\text{Co}_3\text{Pt}$  and (b)  $\text{CoPt}_3$  films obtained at -1.1 and 1.0 V, respectively, on the Si/Ti (15 nm)/Au (100 nm) substrates at 25 °C after circulating 1.6  $\text{C}\cdot\text{cm}^{-2}$  in (A) aqueous solution, (B) micellar solution, and (C) IL/W microemulsion. Aqueous solution composition component: (a) 10 mM  $\text{Na}_2\text{PtCl}_6$  + 10 mM  $\text{CoCl}_2$  and (b) 16 mM  $\text{Na}_2\text{PtCl}_6$  + 4 mM  $\text{CoCl}_2$  solutions, respectively.

- <sup>a.</sup> Grup d'Electrodeposició de Capes Primes i Nanoestructures (GE-CPN), Departament de Química Física and Institut de Nanociència i Nanotecnologia (IN<sup>2</sup>UB), Universitat de Barcelona, Martí i Franquès 1, E-08028, Barcelona, Catalonia, Spain.
- <sup>b.</sup> National Research Centre "Kurchatov Institute", B.P. Konstantinov Petersburg Nuclear Physics Institute, 188300 Gatchina, Russia.
- <sup>c.</sup> Catalan Institute of Nanoscience and Nanotechnology (ICN2), CSIC and The Barcelona Institute of Science and Technology, Campus UAB, Bellaterra, 08193 Barcelona, Spain.
- <sup>d.</sup> ICREA – Institució Catalana de Recerca i Estudis Avançats, Barcelona, Catalonia, Spain.

## Electrosynthesis, characterization and electrocatalytic properties of the reference Pt samples

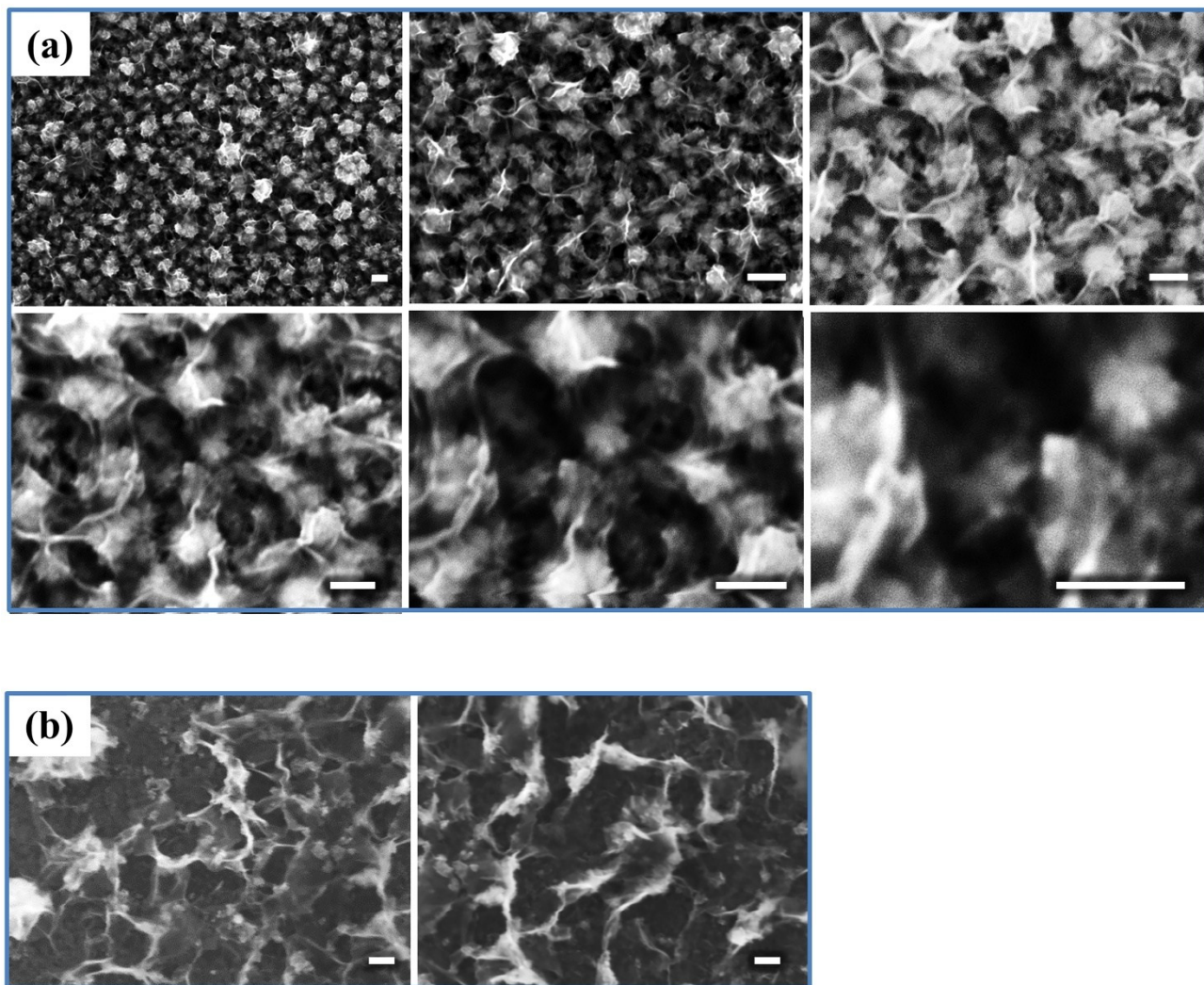
Pt



**Fig. 2S:** (a) Chronoamperometric curves of both aqueous (B) and micellar solutions (A) (both containing 20 mM of  $\text{Na}_2\text{PtCl}_6$ ) obtained at  $-0.2$  V on the Si/Ti (15

nm) /Au (100 nm) substrates after circulating  $1.6 \text{ C}\cdot\text{cm}^{-2}$ . (b) Cyclic voltammetry of compact (B) and mesoporous (A) pure-platinum films in  $\text{H}_2\text{SO}_4$  0.5 M solutions at the scan rate of  $100 \text{ mV s}^{-1}$ . The line corresponds to the 1<sup>st</sup> cycle while the shaded area corresponds 300<sup>th</sup> cycle. Cyclic voltammograms at  $50 \text{ mV s}^{-1}$  (c) and chronoamperometric curves recorded at  $-0.5$  V (d) of compact (B) and mesoporous (A) pure-platinum films in 1M of NaOH + 1 M of  $\text{CH}_3\text{OH}$ . FE-SEM micrographs of as-prepared films - mesoporous (e) and compact (f) and after 300 cycles in 0.5 M of  $\text{H}_2\text{SO}_4$  - mesoporous (g) and compact (h). Scale bar: 40 nm.

## FE-SEM and TEM characterization of mesoporous films

**Co<sub>3</sub>Pt**

**Fig. 3S:** FE-SEM micrographs of Co<sub>3</sub>Pt mesoporous films obtained at -1.1 V on the Si/Ti (15 nm) /Au (100 nm) substrates at 25 °C after circulating (a) 1.6 and (b) 0.4 C·cm<sup>-2</sup> in the IL/W microemulsion. Scale bar: 40 nm.

---

**CoPt<sub>3</sub>**

---

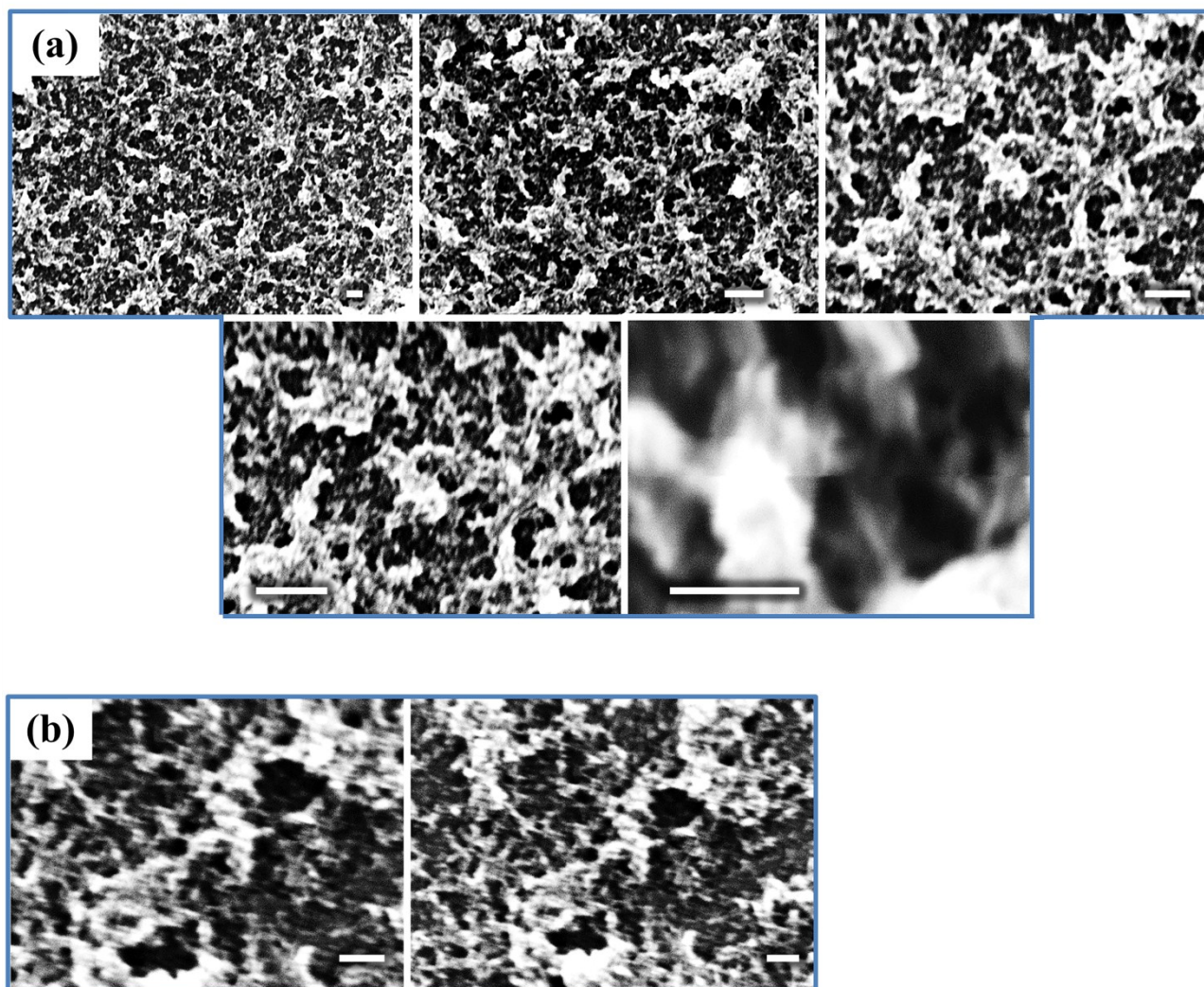


**Fig. 4S:** FE-SEM micrographs of CoPt<sub>3</sub> mesoporous films obtained at -1.0 V on the Si/Ti (15 nm) /Au (100 nm) substrates at 25 °C after circulating (a) 1.6 and (b) 0.4 C·cm<sup>-2</sup> in the IL/W microemulsion. Scale bar: 40 nm.

## XPS spectrum of the mesoporous Co-Pt alloys

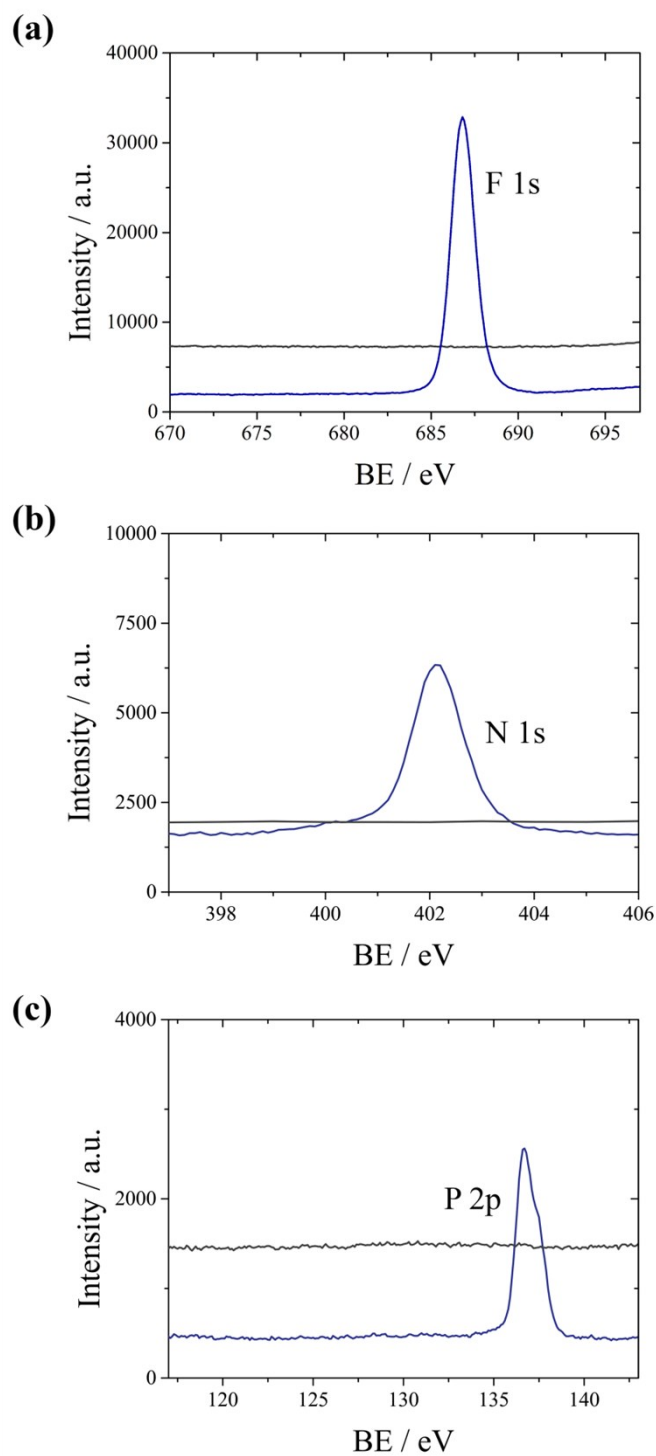
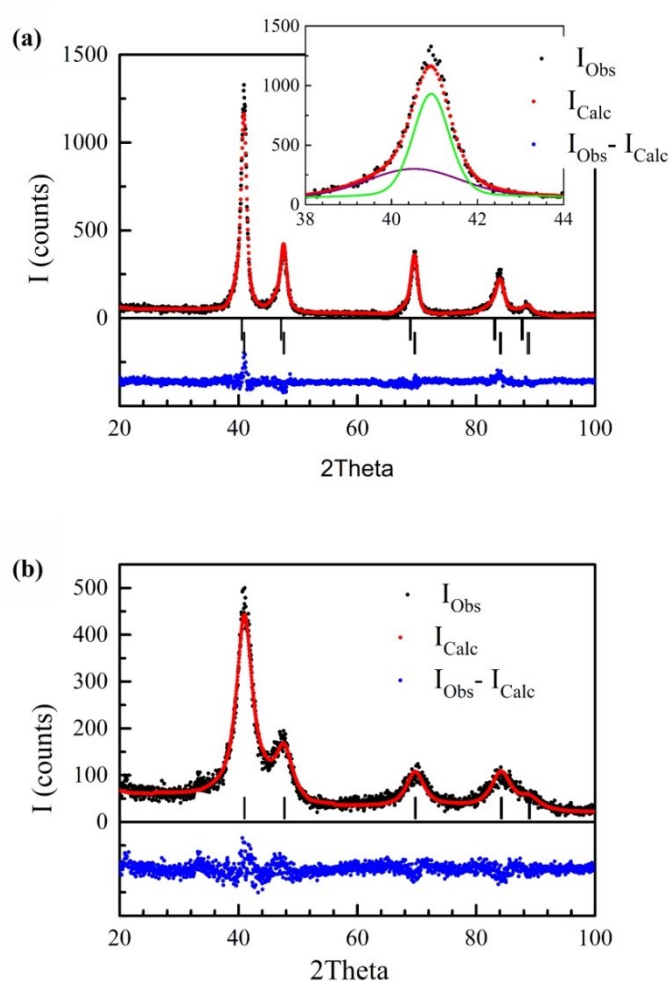


Fig. 5S: (a) F 1s, (b) N 1s and (c) P 2p XPS spectra of cleaned (gray) and non-cleaned (blue) mesoporous films.

## X-Ray diffraction

The fact that in all x-ray patterns the reflections have only odd or even ( $hkl$ ) values indicates that the samples present a face centered cubic ( $fcc$ ) structure (see Fig. 7S). Moreover, the absence of the (100) and (110) reflections reveals that Co and Pt are uniformly distributed through all sites forming a chemically disordered lattice, indicating a  $Fm\bar{3}m$  space group rather than  $Pm\bar{3}m$  or  $P4/mmm$ , which correspond to the ordered  $Co_3Pt$  or  $PtCo_3$  structures. The lattice parameters are comprised between the  $fcc$  Co (3.54 Å) and  $fcc$  Pt (3.92 Å), and they mostly cluster between 3.668 and 3.899 Å. However, some of the structures (particularly the compact films) are not single phase (see Fig. 7Sa), but present additional phases with the same structure, but with different lattice parameters and sizes (see Table 1S). This may explain the spread of lattice parameters, although the different amount of defects in the diverse films may also contribute to the differences in the lattice parameters. In fact, the slight variation of the lattice parameters in the



**Fig. 6S.** Fitted XRD patterns for the mesoporous (a)  $CoPt_3$  and (b)  $Co_3Pt$  samples. Shown in the inset of (a) is an enlarged view of the (100) peak showing the two components of the fit.

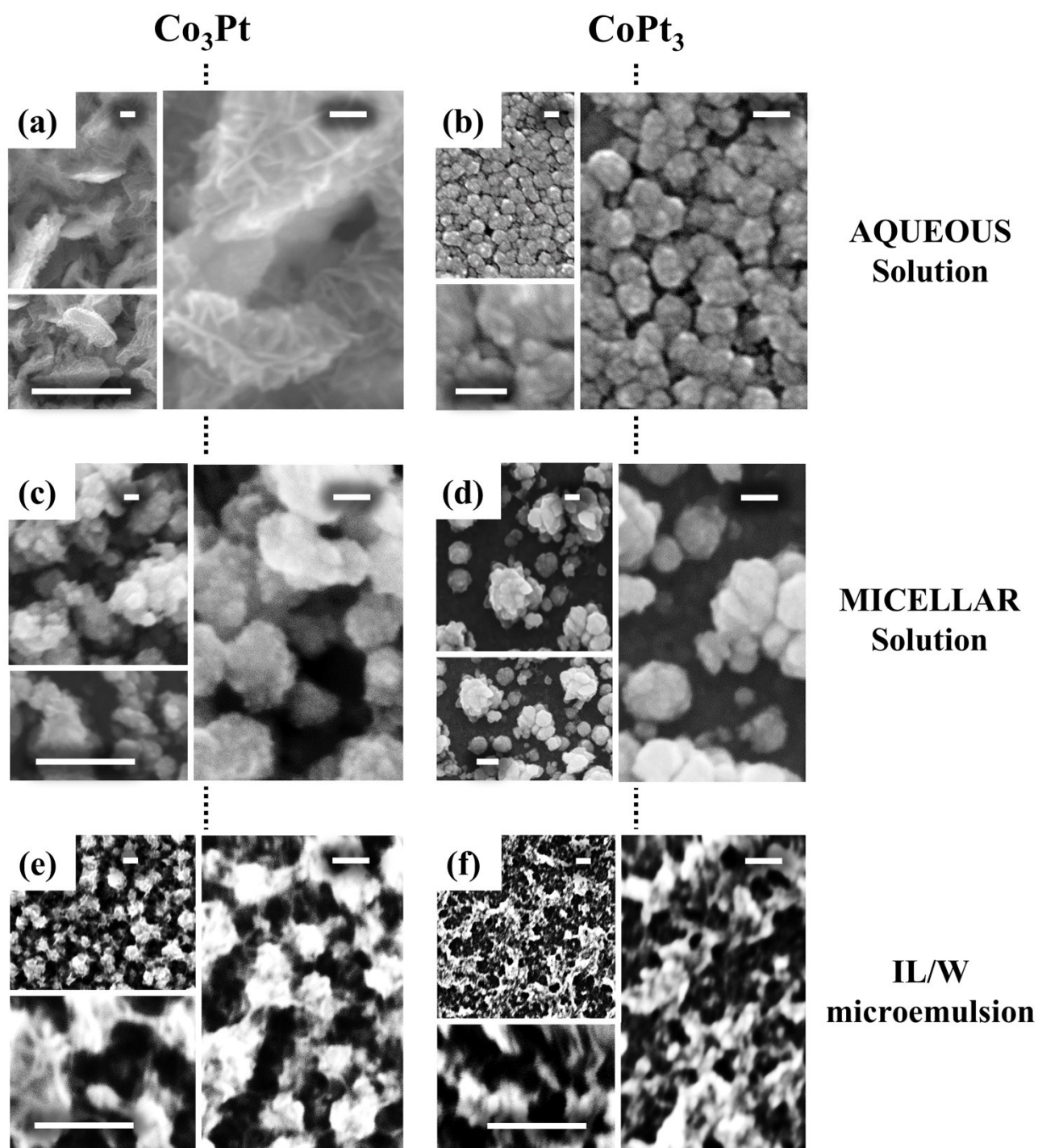
deposits can be justified by the deposition conditions, where the lack of stirring of the solution during the growth of the films can induce small variations of its composition throughout the thickness. Therefore, some small differences in the parameters of the same crystal structure. This is more evident in the compact films, due to the higher deposition rate.

All the samples have relatively small crystallite sizes (Table 1S), although the compact films comprise phases with somewhat larger crystallite sizes (10.7 nm and 7.9 nm for  $\text{CoPt}_3$  and  $\text{Co}_3\text{Pt}$ , respectively), while the nanopowdered ones have relatively smaller ones (2.2 nm and 2.1 nm for  $\text{CoPt}_3$  and  $\text{Co}_3\text{Pt}$ , respectively). On the other hand, the  $\text{CoPt}_3$  mesoporous sample has a crystallite size clearly larger (11.3 nm) than the  $\text{Co}_3\text{Pt}$  one (2.1 nm). Moreover, the films present different preferential orientation (i.e., texture), although there seems to be no clear correlation between the composition or the morphology and the texture (Table 1S).

Finally, note that the parameters have been obtained using the simplest possible model of two-phases, although more complex scenarios, like compositional gradients, might be possible.

		Lattice parameter (Å)	Crystallite size (nm)	Texture
Compact	$\text{Co}_3\text{Pt}$	3.794(2) – 66% 3.825(2) – 34%	7.9(0.5) 2.7(0.3)	111
	$\text{CoPt}_3$	3.812(2) – 53% 3.856(2) – 47%	10.7(0.5) 4.2(0.3)	100
Nanopowder	$\text{Co}_3\text{Pt}$	3.824(2)	2.1(0.3)	100
	$\text{CoPt}_3$	3.709(7)	2.2(0.3)	100
Mesoporous	$\text{Co}_3\text{Pt}$	3.813(2)	2.1(0.3)	111
	$\text{CoPt}_3$	3.820(2) – 73% 3.856(2) – 27%	11.3(0.5) 3.7(0.3)	110

**Table 1S.** Microstructural parameters obtained from the Rietveld refinement of the XRD patterns. Given in brackets is the statistical error.

**FE-SEM characterization of the films after successive acidic and alkaline treatment****Fig. 7S:** FE-SEM micrographs of Co-Pt structures prepared on Si / Ti (15 nm) / Au (100 nm) substrates using aqueous solutions (a, b),

micellar solutions (c, d) or IL/W microemulsion (e, f) after 300 cycles in alkaline media. Scale bar: 50 nm.

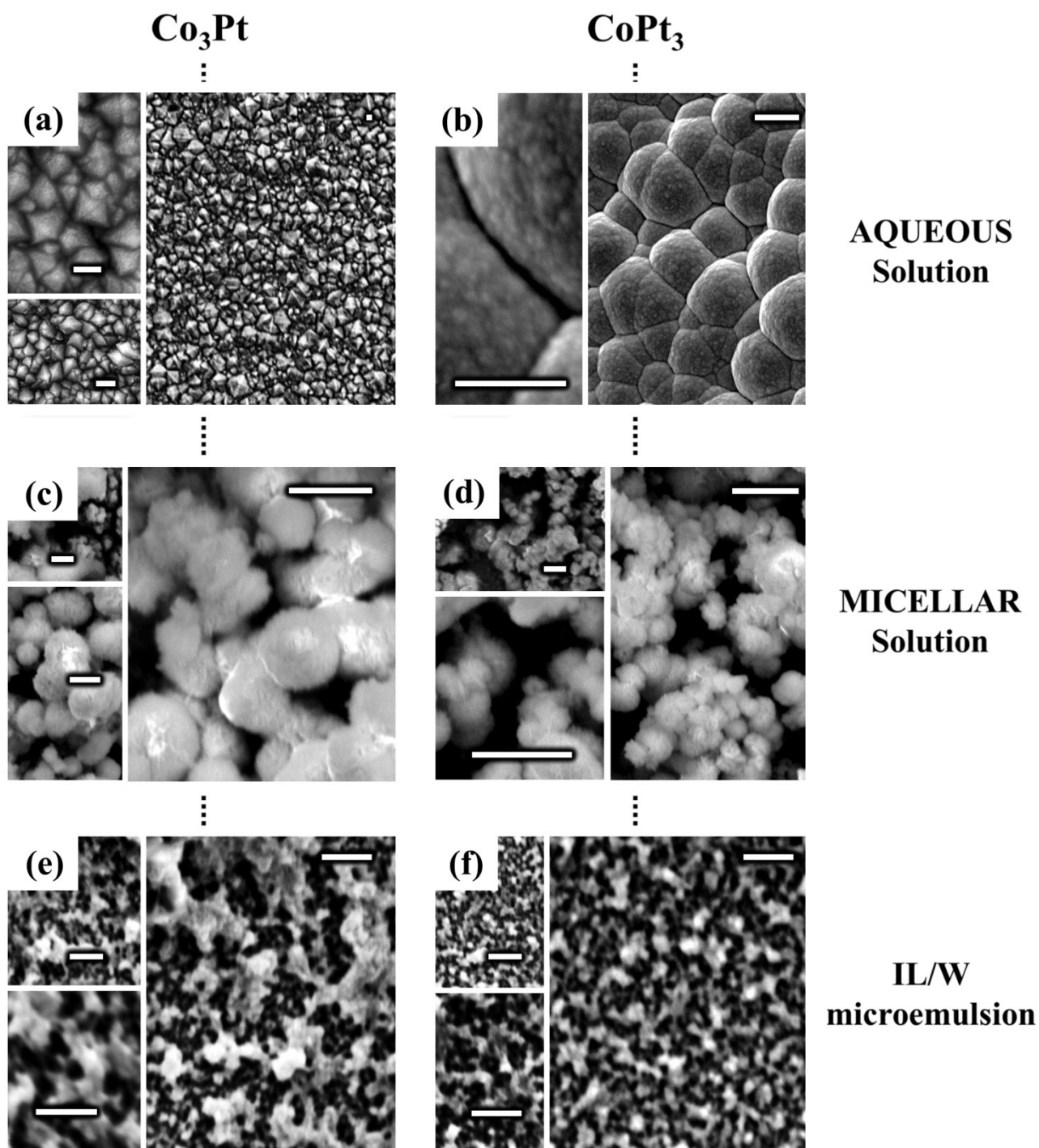


**Fig. 8S:** FE-SEM micrographs of Co-Pt structures prepared on Si / Ti (15 nm) / Au (100 nm) substrates using aqueous solutions (a, b), micellar solutions (c, d) or IL/W microemulsion (e, f) after 10,000 cycles in alkaline media. Scale bar: 50 nm.

### Magnetic manipulation of the detached mesoporous films

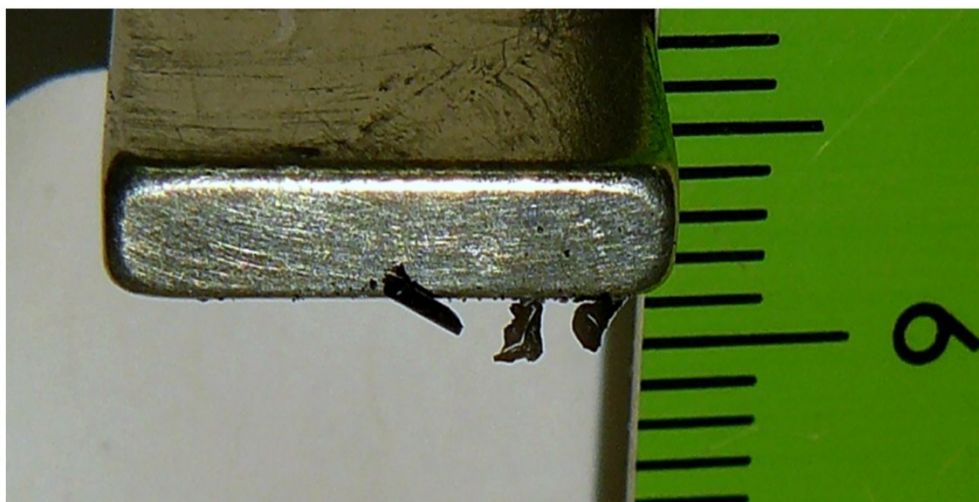


**Fig. 9S:** Flakes of the  $\text{Co}_3\text{Pt}$  mesoporous sample collected by a laboratory FeNdB magnet after being deliberately detached from the substrate, by dipping the film in liquid nitrogen and quickly warming it to room temperature several times (i.e., thermal shock).

## Magnetic properties

The compact films of both  $\text{Co}_3\text{Pt}$  and  $\text{CoPt}_3$  have a typical behavior of polycrystalline thin layers, where the properties are dominated by the shape anisotropy. Namely, the easy magnetization axis (with high squareness, remanent magnetization/saturation magnetization,  $M_R/M_S$ ) is along the plane of the sample, while the hard axis is perpendicular to the film plane (Fig. 11Sa, b). The slightly larger coercivity,  $H_C$ , of the  $\text{CoPt}_3$  sample is expected from higher anisotropy,  $K$ , and lower  $M_S$  ( $H_C \propto K/M_S$ ) characteristic of disordered (fcc)  $\text{Co}_{1-x}\text{Pt}_x$  for high Pt contents.<sup>1</sup> The nanopowdered films have a less well-defined anisotropy, particularly in the case of  $\text{Co}_3\text{Pt}$  where no clear easy axis can be observed (Fig. 11Sc, d), as expected from the disordered arrangement of the particles. In the nanopowder case the properties are probably determined by a combination of exchange and dipolar interactions between the particles. Thus, the random orientation of the particles makes a more quantitative analysis of the results rather complex. Similarly to the nanopowder sample, the mesoporous  $\text{Co}_3\text{Pt}$  film does not have a well-defined easy axis either (Fig. 11Se), as expected from its random arrangement. However, in this case since, contrary to the nanopowder, the whole structure is interconnected, hence, exchange probably dominates the magnetic properties. In fact, due to the reduced crystallite size compared to the compact films, the lower  $H_C$  observed in this case could be related to the random anisotropy model.<sup>2</sup> That is, when the crystallites are very small (smaller than the exchange length,  $l_{\text{ex}}$ ) and exchange coupled but oriented at random the magnetization can no longer follow the easy axis of the grains and the effective anisotropy is reduced, leading to a  $H_C$  decrease.<sup>2</sup> In contrast, the mesoporous  $\text{CoPt}_3$  layer seems to have a superparamagnetic behavior at room temperature (Fig. 11Sf), perhaps due to the rather thin walls of the mesoporous structure. Although, one cannot rule out a very soft behavior ( $H_C < 5\text{-}10$  Oe – difficult to measure using SQUID magnetometer) again due to the random anisotropy model since given the rather low  $M_S$  of  $\text{CoPt}_3$  a rather large  $l_{\text{ex}}$  (much larger than for  $\text{Co}_3\text{Pt}$ ) is expected. A large  $l_{\text{ex}}$  would imply a much more effective averaging of  $K$ , leading to a very small effective  $K$  and hence a low  $H_C$ . However, given the two-phase character of the mesoporous  $\text{CoPt}_3$  sample a more in-depth analysis is not straight forward.



## Electrocatalytic performance (referred to geometrical area)

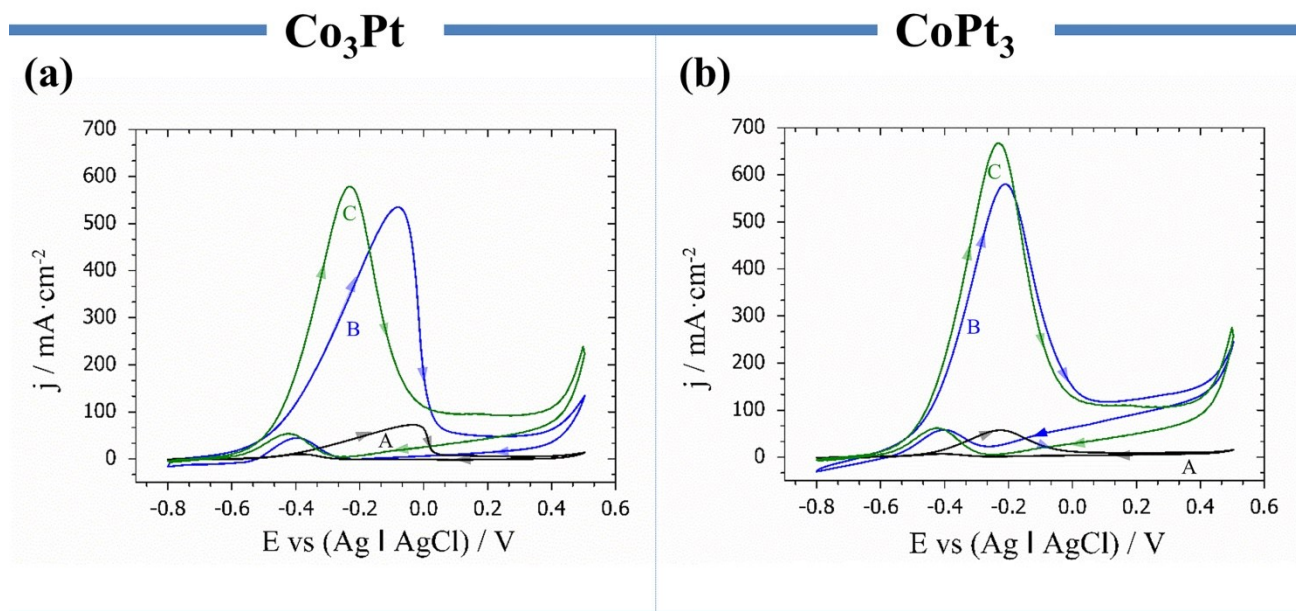


**Fig. 11S:** Cyclic voltammograms at 50 mV s<sup>-1</sup> (a, b) of Co-Pt compact (A), nanopowdered (B) and mesoporous (C) films in 1M of NaOH + 1 M of CH<sub>3</sub>OH normalized by geometrical area.

## Notes and references

1. D. Weller, H. Brändle, G. Gorman, C.J. Lin, and H. Notarys, *Appl. Phys. Lett.* 1992, **61**, 2726.
2. G. Herzer, *IEEE Trans. Magn.* 1990, **26**, 1397.